

Photoluminescence studies of the 1.911-eV Cu-related complex in GaP

H. P. Gislason and B. Monemar

University of Lund, Department of Solid State Physics, Box 725, S-220 07 Lund 7, Sweden

P. J. Dean and D. C. Herbert

Royal Signal and Radar Establishment, St. Andrews Road, Great Malvern, Worcestershire, VR14 3PS, England

S. Depinna, B. C. Cavenett, and N. Killoran

Department of Physics, University of Hull, HU6 7RX, England

(Received 23 February 1982)

The optical properties of the 1.911-eV bound exciton (BE) in Cu-doped GaP have been investigated with several photoluminescence techniques. Photoluminescence (PL) and photoluminescence excitation (PLE) data at different temperatures are combined with magneto-optical data from Zeeman and high-resolution optically detected magnetic resonance (ODMR) measurements. The doping conditions required for this BE spectrum to appear, as well as isotope experiments, prove that the defect binding the exciton involves Cu. A neutral and isoelectronic complex is suggested, most probably a linear Cu-Ga associate with a $\langle 100 \rangle$ -oriented symmetry axis as determined from ODMR data. The axial compressional strain field consistent with this defect geometry completely decouples the spin-orbit coupling of the bound-hole states, leaving pure-spin hole states with lowest energy. The combination of two pure-spin particles accounts for the $J=1$ spin-triplet and $J=0$ singlet states for the bound exciton. The spin-forbidden transition from the $J=1$ triplet to the spin-free ($J=0$) ground state is the 1.911-eV transition clearly resolved in the emission spectrum at low temperatures, while the $J=0$ BE state is observable at 2.002 eV in PLE. The extraordinary large exchange splitting of 91 meV is related to the unusual degree of BE localization. Both particles of the exciton are tightly bound, as supported by measurements of the activation energy for the thermal quenching of the 1.911-eV emission. We interpret this tight binding of both particles as a recently recognized but probably general property of an exciton bound to an associate with an attractive localized potential for holes as well as for electrons. In the present case, the hole is bound in the strong central-cell potential of Cu_{Ga} , while the electron also experiences a strong short-range component of binding potential arising from the effect of the local compressive strain field on the lowest conduction band in GaP. A splitting of hole states in the axial field of the defect is estimated to about 280 meV, exceeding the spin-orbit splitting by at least 200 meV.

I. INTRODUCTION

Many impurities and lattice defects are known to cause deep levels in semiconductors but very few have been positively identified as to their detailed local lattice arrangement.¹ Cu is known to diffuse rapidly into most semiconducting materials at normal processing temperatures and it causes a large number of deep-level defects in, e.g., Si (Ref. 2), GaAs (Ref. 3), and GaP (Ref. 4). Some of these are believed to cause severe problems in devices, e.g., degradation of device performance.⁵ It seems

that the class of defects usually called complexes, i.e., composed of at least two atoms or lattice-point defects is very common in semiconductors. Particularly when the constituent elements of the complex carry opposite charges relative to the host lattice, such defects are favored by pairing under the long-range Coulomb potential upon cooldown after growth or heat treatments.⁶ Such associate types of defects are often neutral and some may be clearly identified as isoelectronic,⁷ in which an impurity or defect molecule is isoelectronic with the host species replaced. A small but significant propor-

tion of these electrically neutral associates introduces into the semiconductor an electronic perturbation sufficiently strong that additional electronic particles may be bound, at least at low temperatures, to form bound excitons. This property makes them particularly accessible to optical studies via photoluminescence techniques,⁸ even for excitons of large localization energies E_{BX} . For neutral associates of the classical isoelectronic type, one electronic particle is frequently bound much more tightly than the other to produce the major part of E_{BX} . This is not an inevitable situation, however, as exemplified by the centers described in this paper. It is relatively difficult to study these neutral associates with standard junction space-charge techniques, such as deep-level transient spectroscopy,⁹ owing to low sensitivity.¹⁰ Since defects of this class are often able to capture both electrons and holes, they may be important excess-carrier recombination centers, and are therefore of great practical interest.

In this paper we report an optical investigation of a deep Cu-related center in GaP, binding an exciton which has the lowest electronic excitation energy at 1.911 eV at 2 K. This center is introduced by diffusion at temperatures 1000–1100°C, followed by rapid quenching to room temperature. Several other bound excitons are observed as a result of such Cu diffusion, the most prominent being the characteristic orange-luminescence (COL) emission with a lowest electronic line at 2.1774 eV at 2 K.¹¹ For the 1.911-eV center it has been possible to carry out a complete optical study to identify the defect symmetry and the electronic properties. From a combination of photoluminescence emission spectra (PL) and excitation spectra (PLE) with magneto-optical data from optically detected magnetic resonance (ODMR), a tentative identification of the 1.911-eV defect as a neutral $\langle 100 \rangle$ -oriented Cu-Ga associate is suggested but other models are discussed as well. Preliminary results from the ODMR investigations have already been published separately.¹² These results show that the lowest bound-exciton state is a nearly-pure-spin triplet, in agreement with earlier Zeeman measurements.⁸ While Zeeman data only showed an isotropic triplet splitting, from ODMR measurements it was also possible to establish the defect orientation firmly. The triplet configuration suggests that the center binding the exciton lowers the symmetry of the GaP lattice with a particular sign of the local perturbation of the host states. The presence of higher electronic states, split off from the lowest

bound-exciton state by several tenths of an eV, together with the large activation energy for thermal quenching of the emission, suggests that both the electron and the hole are fairly strongly bound in the case of the 1.911-eV center. As already mentioned, this situation creates quite different bound-exciton states than the previously studied complexes of nitrogen pairs¹³ or Cd-O and Zn-O pairs in GaP,^{14,15} where one of the particles (the hole) can be described as bound in a shallow state (about 40 meV) merely by the Coulomb potential of the more tightly bound electron.¹⁶ In addition, the local perturbation of the GaP host states has opposite sign to that reported here. We believe that the results obtained here for the electronic structure of these deeply bound Cu-related exciton states are very helpful in the development of a theoretical understanding of the general range of behavior possible for deep-level complexes in semiconductors.

In Sec. II the procedures for material preparation and doping required to obtain the copper-related defects are described. The experimental techniques in the optical measurements are also briefly discussed.

Section III A includes photoluminescence data for the 1.911-eV center at 2 K. At low temperatures a detailed structure due to phonon replicas is observed in the emission. Several of these phonon modes show isotope shifts when ⁶³Cu is replaced by ⁶⁵Cu. In Sec. III B the spectral evolution at elevated temperatures is shown over a wide temperature range. Also the thermal quenching of PL emission intensity is documented up to 130 K, where the emission disappears.

In Sec. IV selective absorption data are presented for the 1.911-eV defect obtained from PLE with a cw dye laser. In addition to the lowest bound-exciton state several excited configurations are revealed, with much larger oscillator strength than the lowest triplet state. These excited states were only observed in PLE since the energy separations involved are much too large to permit significant thermal population as required for their observation in photoluminescence at higher temperatures.

Section V contains a full description of the ODMR data for the 1.911-eV center. This is the first case where a bound exciton could be studied in detail by ODMR in a III-V compound, and very good data are obtained owing to the unusually high sensitivity of ODMR in this case.

A specific model for the electronic properties of the center is presented under the discussion in Sec. VI. The information on the defect symmetry

(ODMR) suggests a dominant $\langle 100 \rangle$ -oriented compressive axial field. The very large exchange splitting determined from PLE indicates a much greater electron-hole overlap than in previously studied cases of bound excitons in GaP.¹⁷

II. SAMPLE PREPARATION AND EXPERIMENTAL PROCEDURE

The Cu-doped GaP samples used for this investigation were all diffused with Cu at high temperatures. It was found that material doped with Cu during growth from Ga solutions cooled from 1100 to 800 °C (without diffusion) did not show strongly the photoluminescence bound-exciton spectra reported here. Rather, other broad emissions were then present, which indicates that different Cu defects were preferably created. The diffusion procedure used to create a strong 1.911-eV emission was to evaporate Cu onto a GaP slice (epitaxial or bulk) and use an evacuated ampoule, backfilled with dry N₂ gas and with an equilibrated GaP-Ga melt adjusted to the employed diffusion temperature. Excess Cu was also placed in contact with the melt. Suitable diffusion temperatures were 1000–1100 °C, the diffusion time was typically 1 h, and the samples were rapidly quenched to room temperature after the diffusion. It was found that no major difference in the intensity of the 1.911-eV PL emission occurs with doping and similar intensities were found after diffusion into strongly *n*-type, nominally undoped and Zn-doped *p*-type wafers. Also the 1.911-eV spectrum could be produced easily in both bulk and liquid-phase epitaxy GaP material.

For the photoluminescence measurements an Ar⁺ laser, sometimes in combination with a tunable cw dye laser, was employed. Emission spectra and excitation spectra could be recorded from 1.8 up to 130 K at well-regulated temperatures. A double Jarrel-Ash 0.75 grating monochromator was used for obtaining emission spectra, and also on the detection side for dye-laser-excited excitation spectra. Zeeman data of the 1.911-eV line in photoluminescence reported here were obtained at the Royal Signal and Radar Establishment with a 3.5-T Varian electromagnet and at Hull University with a Thor superconducting magnet at fields up to 6 T. Unfortunately, the lifetime broadening of excited states observed in excitation spectra made Zeeman data of these lines impossible to obtain. ODMR data were obtained at Hull University in an X-band system at 2 K, as described elsewhere.¹⁸

A superconducting magnet was employed and the sample could be rotated within the rectangular cavity by a gear arrangement to obtain the angular dependence of the ODMR signal.

III. EXPERIMENTAL RESULTS

A. Emission spectra

The high-energy part of the photoluminescence spectrum of Cu-diffused GaP recorded at 1.8 K is shown in Fig. 1. The spectrum is dominated by the so-called COL emission¹¹ with a sharp electronic transition at 2.1774 eV. The COL center has recently been identified as a neutral Cu associate in GaP and its properties are discussed elsewhere.^{11,19–22} On the low-energy tail of the COL emission a second Cu-related spectrum is present (Fig. 1). Both these transitions are characterized by a very long decay time, on the order of 100

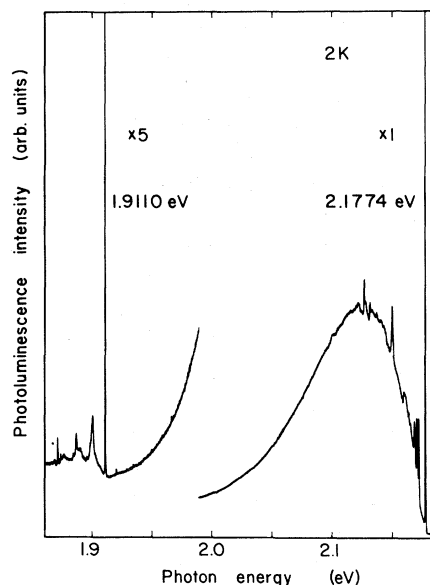


FIG. 1. Two dominant bound-exciton photoluminescence bands typical of GaP diffused with Cu at 1050 °C, recorded at 1.8 K. The spectrum is not corrected for monochromator and photomultiplier response curves. The stronger emission at higher photon energy is the so-called COL bound-exciton emission with lowest electronic line at 2.1774 eV (Ref. 11). The intensity of the low-energy spectrum with electronic line at 1.911 eV is uncorrelated to the intensity of the COL emission. Sometimes the 1.911-eV spectrum is absent indicating a more critical doping procedure. Both transitions have a very long decay time for a BE in GaP, about 100 μ s.

μs .^{20,22} A sharp electronic line at 1.911 eV is characteristic for the low-energy emission as shown in more detail in Fig. 2. This line is found to split into a nearly isotropic triplet in a magnetic field (Fig. 2). In addition, a structured phonon sideband is present at lower photon energies with phonon energies as listed in Table I. The most prominent phonon replicas are labeled in Fig. 2 as B_1 at 10.3 meV, B_5 at 24.2 meV, and B_9 at 39.9 meV below the no-phonon line. This last mode is a local-gap mode, frequently seen in other bound-exciton spectra in GaP.^{11,23,24} A remarkably low intensity is observed for phonon modes in the optical energy range between 45 and 50 meV. Thus the sharp TO_Γ and LO_Γ replicas are not resolved clearly but instead a broad structure in the energy range of LO_Γ is present in Fig. 2. Coupling to true local modes, that is phonon modes above the highest phonon energy of the GaP host lattice, seems absent. This indicates that the complex binding the 1.911-eV exciton does not contain any atoms lighter than the host species replaced.

Several of the discrete phonon replicas show a sizable isotope shift upon substitution of ^{63}Cu with ^{65}Cu as listed in Table I. Only a very small shift is observed for the electronic line, however. The low-energy quasilocalized phonon mode B_1 at 10.3 meV might account for the major part of the phonon sideband through a coupling constant $S \approx 1$. The broad peak at about 22 meV then is the second replica, whereas the third and fourth replicas appear at about 34 and 48 meV, illustrating anharmonic effects in the final vibronic state of the transition. This low-energy phonon mode B_1 is also present at elevated temperatures on the anti-Stokes wing. The first anti-Stokes replica is clearly resolved at temperatures above 25 K, showing phonon energies reduced by about 10% in the excited electronic bound electron (BE) state compared with the ground state (Fig. 3). The interpretation of the phonon sideband of the 1.911-eV emission as being mainly composed of multiphonon replicas of a single 10-meV mode with sharper discrete structure superimposed is even more appealing with rising temperature, when this discrete structure becomes smeared out. Then the spectrum can be viewed as consisting only of these broad replicas at about 10-meV intervals, following the no-phonon line.

The different crystals used in this investigation often show weaker sharp lines 9.2, 23, and 38 meV above the 1.911-eV electronic line. Occasionally these extra emission lines are absent, and their intensities do not correlate with the 1.911-eV emis-

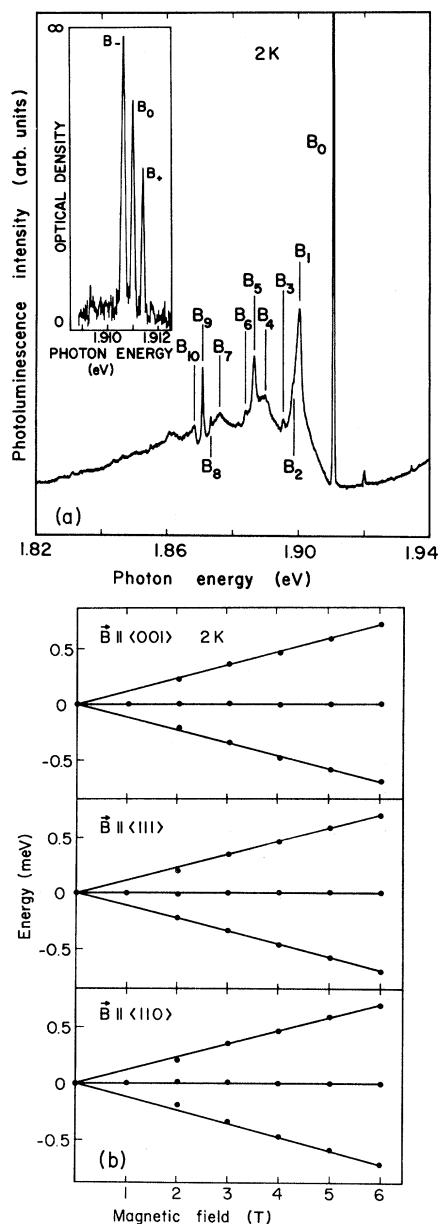


FIG. 2 (a) Photoluminescence spectrum of the 1.911-eV bound-exciton emission for the same Cu-diffused GaP sample as in Fig. 1, recorded at 1.8 K. The excitation wavelength is 5145 Å. The electronic line at 1.911 eV is a spin-forbidden transition from a $J=1$ triplet to the spin-free final state of an isoelectronic associate. On the inset is shown the essentially symmetric splitting of this line into three components in magnetic field, $B=3.4$ T, $\vec{B} \parallel [100]$. This splitting corresponds to $g \approx 2.0$ and the thermalization shows that the splitting occurs in the initial state of the luminescence transition. (b) Splitting of the 1.911-eV emission line in magnetic field up to 6 T. Three different orientations of the field are shown, $\vec{B} \parallel \langle 001 \rangle$, $\vec{B} \parallel \langle 111 \rangle$, and $\vec{B} \parallel \langle 110 \rangle$. All show similar isotropic splitting.

TABLE I. Phonon energies from the sideband of the 1.911-eV luminescence spectrum in Fig. 2.

Notation	Phonon energy meV	ΔE (^{63}Cu - ^{65}Cu) meV	Interpretation
B_1	10.3	0	
B_2	12.4	0	
B_3	15.4	0.2	
B_4	20.9	0.2	
$2B_1$	22.0		Second replica of B_1
B_5	24.2	0.5	Distorted LA mode
B_6	26.9	0.3	
$3B_1(B_7)$	34.8	0	Third replica of B_1
B_8	37.4	0	Local gap mode
B_9	39.9	0.1	Local gap mode
B_{10}	42.5	0	

sion. Consequently these lines are not directly related to the 1.911-eV emission, but rather to an independent emission from an unknown center. To illustrate this situation the spectrum of a crystal different from the one used in Fig. 2 is shown in Fig. 4. Here the line at 1.9202 eV is about half as strong as the 1.911 line when excited with above-band-gap excitation (5145 Å). When excited in the

strong 2.002-eV absorption line observed selectively for the 1.911-eV emission in PLE measurements (see Sec. IV), the 1.9202-eV line does not show a

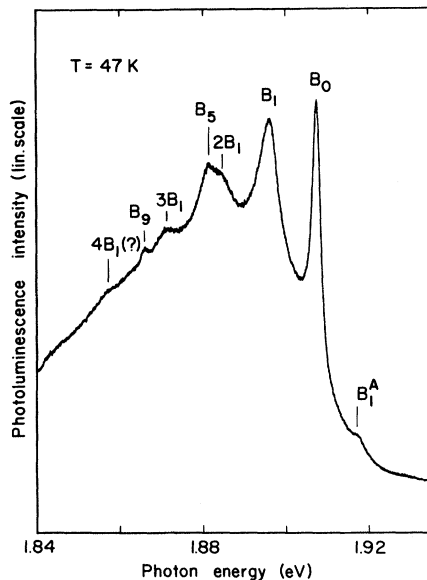


FIG. 3. Portion of the photoluminescence spectrum for the same crystal as in Fig. 2, recorded at 47 K. An anti-Stokes component of the phonon mode B_1 about 9 meV above the reduced no-phonon line first appears at 25 K. The phonon energy in the excited vibronic state is reduced by about 10% compared with the ground state.

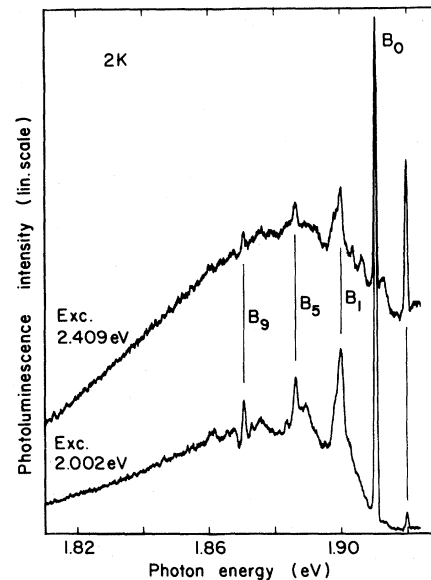


FIG. 4. Photoluminescence spectrum for a Cu-diffused GaP sample, different from the one used in Figs. 1 and 2. The upper curve shows a transition at 1.9202 eV, which is nearly equally strong as the 1.911-eV transition in this sample, when excited above the band gap at 5145 Å. The phonon replicas of this line dominate the phonon sideband, which has a different shape from the sideband in Fig. 2. When exciting with a cw dye laser in the strong 2.002-eV absorption line observed in PLE, only the 1.911-eV line and the corresponding phonon replicas are selectively enhanced, giving the familiar spectral shape shown in the lower curve.

resonant enhancement of the intensity as the 1.911-eV line does. The 1.911-eV line now dominates over the higher one and its characteristic phonon sideband is revealed. This procedure proves that the lines in fact belong to different centers.

B. Temperature dependence of the 1.911-eV luminescence

As already mentioned, the phonon coupling of the 1.911-eV electronic line is dominated by coupling to a single quasiloalized mode of about 10 meV, giving the structured emission spectrum shown in Fig. 2 at low temperatures. The coupling strength for this emission is rather weak. The Huang-Rhys factor S , evaluated from the ratio between the integrated intensities of the zero-phonon line and the total emission according to the equation $I_0/I = \exp(-S)$ (Ref. 25) gives $S \approx 2$. This is considerably smaller than in the case of the COL emission where $S \approx 5$ (Ref. 19) (cf. Fig. 1).

The electronic line of the 1.911-eV emission is clearly visible as a discrete peak up to about 80 K, although drastically smeared out as shown in Fig. 5. About 80 K the no-phonon line can still be easily distinguished as a broad shoulder at photon energies between the increasing anti-Stokes wing and the envelope showing faintly the broad 10-meV phonon replicas. At 100 K this structure disappears together with the no-phonon line, leaving a smooth emission envelope. In contrast to the COL which shows a strong coupling to low-energy modes, both discrete and continuous, this behavior is typical for a weaker coupling to the low-energy parts of the continuous acoustic phonon bands. The no-phonon line vanishes in the COL emission at much lower temperature or just above 40 K.¹⁹

A marked increase in the background intensity is observed at temperatures above 100 K, where the remaining intensity of the 1.911-eV emission appears superimposed on a broad emission extending from about 2 eV down to below 1.8 eV, with its maximum around 1.9 eV. This background was subtracted when evaluating the curve in Fig. 6, which shows the temperature dependence of the total-emission intensity for the 1.911-eV emission. Only a slight decrease of the intensity (within 15–20%) is observed in the low-temperature region up to about 80 K. This decrease may be partly overvalued due to difficulties in separating the electronic quenching for such a structured emission from vibrational broadening effects, which con-

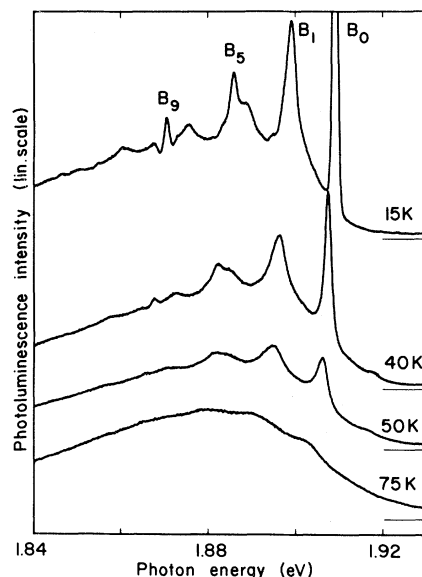


FIG. 5. Spectral evolution of the 1.911-eV emission band with rising temperature. The electronic line is visible up to about 100 K, where all structure vanishes, although it is very much smeared out above 80 K. At this temperature the phonon sideband clearly consists of replicas of the electronic line with a dominating 10-meV phonon mode. This same mode is also observed on the anti-Stokes wing. The total intensity of the emission is not affected much until above 80 K.

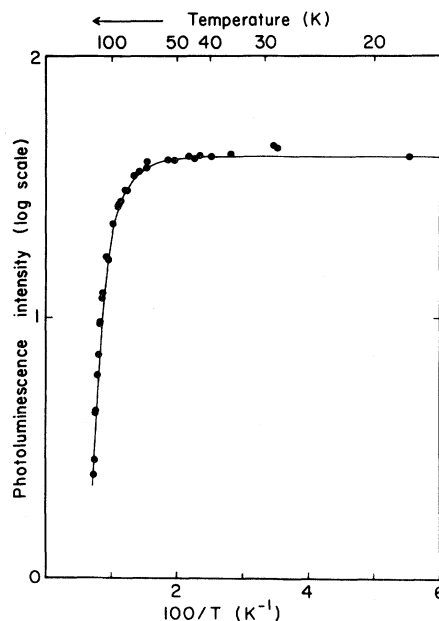


FIG. 6. Temperature dependence of the total-emission intensity for the 1.911-eV emission taken with extrinsic excitation at 2.03 eV. The thermal activation energy as the emission rapidly disappears in the temperature range 100–130 K is $E_1 = 120 \pm 10$ meV. The smaller decrease before the final step corresponds to a second activation energy $E_2 = 30 \pm 5$ meV.

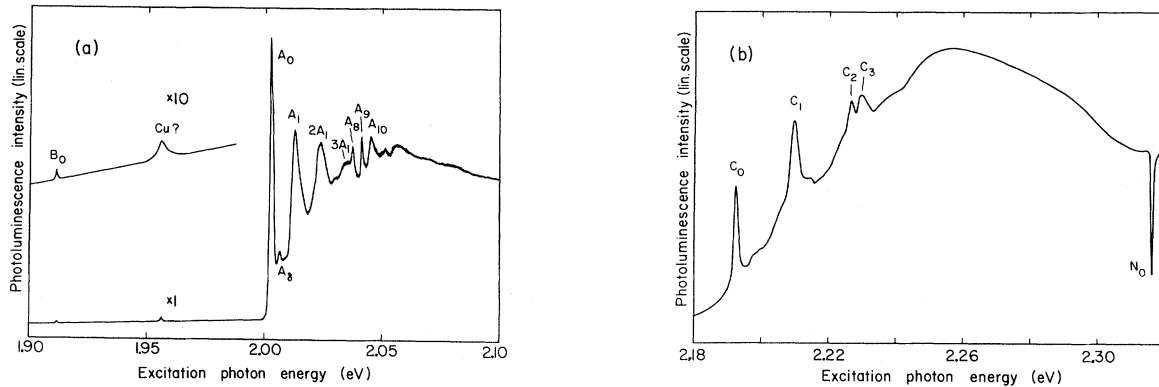


FIG. 7. Photoluminescence excitation spectrum for the 1.911-eV emission obtained with a tunable cw dye laser at 1.8 K. The detection wavelength is set to 6550 and 6650 Å alternatively, giving identical spectra. The electronic line B_0 at 1.911 eV in (a) is a spin-forbidden triplet transition with a very low oscillator strength, just barely detectable. A dominating electronic line A_0 at 2.002 eV marks the onset of a strong phonon wing, showing general similarities in phonon coupling as for the B_0 emission line at 1.911 eV. The line A_0 is attributed to a $J=0$ singlet BE state and the replicas A_1 – A_7 are manifestations of the same 10-meV phonon mode as in the emission spectrum in Fig. 2.

serve the area under the emission curve. The thermal activation energy observed as the emission envelope rapidly disappears in the temperature range 100–130 K is $E_1 = 120 \pm 10$ meV for extrinsic excitation at 2.03 eV. A second smaller activation energy $E_2 = 30 \pm 5$ meV is deduced from the slope of the gradually decreasing intensity curve before the final step. The overall shape of the quenching curve is described by the expression

$$I(T) = I(0) \left[1 + C_1 \exp \left[-\frac{E_1}{kT} \right] + C_2 \exp \left[-\frac{E_2}{kT} \right] \right]^{-1},$$

where the weighting factors $C_1 = 4 \times 10^5$, $C_2 = 25$ express the relative importance of each step. From the thermal activation energy it can be deduced that the more loosely bound particle has a binding energy of the order of 120 meV. This is a factor 2–3 larger than observed in the case of previously studied excitons bound at isoelectronic centers in GaP.^{13,16} The large binding energy of both electronic particles of the BE causes an unusually strong electron-hole overlap in this case as discussed below.

Measurements with intrinsic excitation at 5145 Å give qualitatively similar results; the discrete structure disappears around 100 K and the emission is undetectable above 130 K. A marked difference though, is a considerably lower activation energy ($E = 50 \pm 5$ meV) than for extrinsic excitation. The curve is described by this slope

alone. Consequently the decrease is more rapid at lower temperatures than in the extrinsic case but slower towards higher temperatures. This difference is very probably due to other effects than thermal release of particles from the 1.911-eV center, relating to the mechanism by which these BE states are created under extrinsic excitation.¹³

IV. PHOTOLUMINESCENCE EXCITATION SPECTRA

In Fig. 7 is shown the low-temperature PLE spectrum of the 1.911-eV emission, obtained with a cw dye laser in the energy range between 1.9 eV and the band gap. The detection monochromator wavelength is selectively set to portions of the emission envelope, alternatively to 6550 and 6650 Å to exclude possible interference with Raman scattering lines. The excitation spectrum consists of a weak electronic line at 1.911 eV, corresponding to the emission line at the same energy. This line has a surprisingly low oscillator strength and is indeed very difficult to detect even with dye laser excitation. Therefore, no clear signs of the structured phonon wing present in emission are seen in the absorption spectrum. However, at 1.956 eV a group of weak and badly resolved lines is seen, the strongest one being a factor of 10–15 stronger than the 1.911-eV triplet. This peak has a linewidth of approximately 1.5 meV, which suggests that it involves a lifetime-broadened excited state. A careful inspection of PLE curves for different crystals shows that this broad feature is con-

nected with a weaker sharp line at 1.949 eV, which is also sometimes seen in emission, although barely detectable. We therefore conclude that these features are not related to the 1.911-eV center, and their appearance in the PLE spectrum is due to a different defect.

At 2.002 eV a strong and broad line A_0 (half-width 2 meV) marks the edge of a richly structured absorption wing extending up to the band-edge region. From the previous discussion it is clear that this strong wing originates from the 1.911-eV emission. When exciting in the 2.002-eV line the 1.911-eV emission is selectively enhanced, and in addition the absorption wing occurs only when detecting this emission. From Fig. 7(a) it is evident that almost the total oscillator strength of the optical transitions related to this bound exciton lies in the higher-energy components starting at 2.002 eV. The relative intensities of the 1.911-eV B_0 line and the strong 2.002-eV component A_0 are about 1:100. This ratio is even lower when the phonon-assisted sidebands are taken into account. The discrete phonon structure connected with the A_0 transition resembles closely the corresponding phonon wing of the 1.911-eV line in emission. This is another strong argument for the identification of the 2.002-eV line as an excited configuration of the bound exciton having its lowest state at 1.911 eV. In Table II the phonon energies from the excitation measurements are listed, the notation referring to the labels in Fig. 2.

The sharp peak at 3.8 meV above the A_0 electronic line does not correspond to any phonon mode in emission. Otherwise the structure largely consists of a strong coupling to a 10-meV phonon mode in a similar way as for the 1.911-eV emission line B_0 . The first replica A_1 , 10.2 meV above A_0 is strongest, while the second one, 21 meV above the A_0 line, is still very distinct. The third replica (33 meV) is merging into the continuum background and partly hidden by the sharp peak A_8 , 34.8 meV above A_0 . A_8 is not represented in the emission spectrum. However, the 37.4-meV B_8 mode is fairly close to the A_8 mode in energy, being a localized-gap mode as well. The energy difference is 2.6 meV between the A_8 and B_8 modes while the A_9 mode of 38.7 meV is 1.2 meV lower in energy than the strong B_9 gap mode of 39.9 meV. On both sides of this mode dips occur in the excitation spectrum in a similar manner as for the emission spectrum. The high-energy shoulder of the dip lies at 42.5 meV which is also the value for the corresponding feature in emission. This is close to the lower edge of the optical density-of-states branch for pure GaP lattice.²⁶

No major discrete peaks occur in the absorption spectrum above 2.10 eV until a strong broadened (half-width about 1 meV) electronic line C_0 appears at 2.1928 eV, more than 0.28 eV above the 1.911-eV ground state [Fig. 7(b)]. Above this line a well-resolved structure has the proper width and energy range to represent phonon replicas of the

TABLE II. Energies of the observed structure in the PLE spectrum of the 1.911-eV emission in Fig. 7.

Notation	Photon energy	Phonon energy	Interpretation
B_0	1.911 eV		$J=1$ BE triplet
A_0	2.002 eV		$J=0$ BE singlet
A_8		3.8	Quasilocalized low-energy mode
A_1		10.2	cf. B_1 in Fig. 2
$2A_1$		21	Second B_1 replica
$3A_1$		33	Third B_1 replica
A_8		34.8	cf. B_8 in Fig. 2
A_9		38.7	cf. B_9 in Fig. 2
A_{10}		42.5	cf. B_{10} in Fig. 2
C_0	2.1928 eV		BE states from split-off hole states (see Fig. 15)
C_1		16.8	Phonon replica of C_0
C_2		34	Local gap mode of C_0
C_3		37.2	Local gap mode of C_0

C_0 line. This excitation structure appears only when the detection wavelength is within the 1.911-eV emission band, which associates it with this Cu center. The strongest peaks are C_1 , a rather broad (2 meV) peak 16.8 meV above C_0 , closely followed by another much weaker one, 4 meV higher in energy. A pair of peaks C_2 and C_3 at 34 and 37.2 meV above C_0 are relatively sharp as expected for localized gap modes, and are therefore most likely phonon replicas of the C_0 electronic line. No further structure is found in the absorption spectrum up to the nitrogen bound-exciton line N_0 , which occurs as a narrow dip in the spectrum. This is in contrast to the COL emission in the same crystals (Fig. 1) which gets a considerable excitation transfer at the N_0 bound-exciton energy.¹¹ No other well-known shallow exciton lines are observed in this excitation spectrum. It is also interesting to note that excitation transfer from the dominating COL spectrum (Fig. 1) in these crystals is apparently very weak and not observed in Fig. 7.

This can be understood in terms of a rather small concentration (probably $< 10^{16} \text{ cm}^{-3}$) for both the COL center and the 1.911-eV center discussed here, and the large exciton localization energy E_{BX} of the COL. Radiation-field transfer will also be poor because of low oscillator strengths of luminescence associated with the B spin-triplet BE states.

In Figure 8 the low-energy part of the PLE spectrum is shown at elevated temperatures. Here, the structure of the phonon sideband due to the dominating 10-meV phonon mode becomes even more pronounced, since sharp features become smeared out at higher temperatures. This is similar to the case of the phonon sideband of the B_0 line in emission.

V. ODMR RESULTS

The experimental technique used in obtaining ODMR data was briefly discussed above under Sec. II. All data discussed here were obtained with the sample immersed in pumped He at 2 K and at X-band (~ 9 GHz) microwave frequencies. For the 1.911-eV emission an unusually strong ODMR signal was observed, since the fraction of the total PL signal that was modulated with the microwave field was as high as 5%. This is fortunate since it makes very detailed and well-resolved resonances obtainable. A preliminary report has been published.¹² An example of typical ODMR signals for the orientation $\vec{k} \parallel \vec{B} \parallel [001]$ is shown in Fig. 9, where resonances in both the circularly polarized

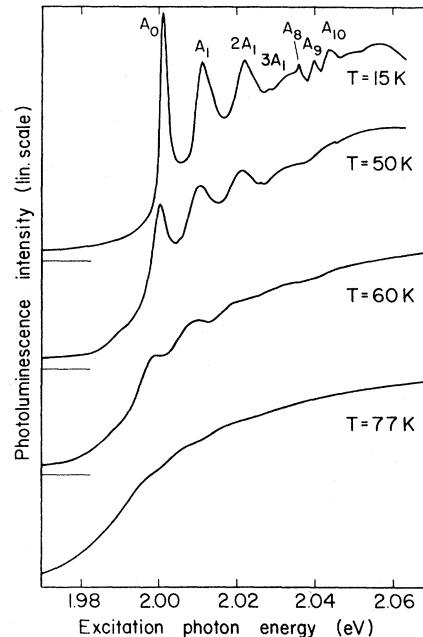


FIG. 8. Portions of PLE spectra for the 1.911-eV emission at several different temperatures. The spectral evolution of the structured absorption band when the temperature is raised is largely similar to the case of emission in Fig. 6. Thus the dominant 10-meV phonon mode is clearly seen at elevated temperatures both on the Stokes and the anti-Stokes wing.

emission components ΔI_{σ^+} (upper) and ΔI_{σ^-} (lower) are shown. Both signals are, in fact, increases in emission intensity, which means that the total emission intensity is also increased by the mi-

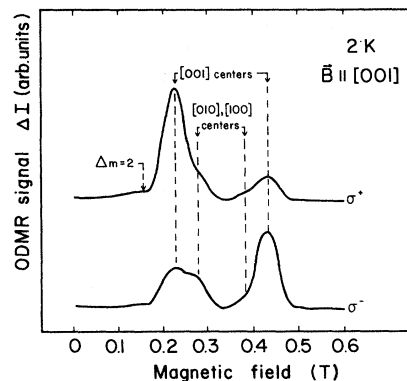


FIG. 9. ODMR signals for $\vec{B} \parallel [001]$ obtained by monitoring ΔI_{σ^+} (upper curve) and ΔI_{σ^-} (lower curve). The spectrum consists of $\Delta M_s = \pm 1$ resonances from the three $\langle 100 \rangle$ centers [001], [010], and [100] as shown and a single $\Delta M_s = \pm 2$ resonance which is approximately the same for each center.

crowave field. This is the usual case when we have an unthermalized or a partly thermalized essentially pure-spin-triplet system, i.e., the emission lifetime τ is shorter than the spin-relaxation time T .¹⁸ Also the observation of pairs of resonances for each axial center with different orientation relative to the $z \equiv [001]$ axis of the experiment is characteristic for a triplet exciton.

The ODMR signal of Fig. 9 was obtained by monitoring a broad spectral range of the emission, with an edge filter cutting out light at wavelengths shorter than 6600 Å to obtain optimum signal-to-noise ratio for a detailed analysis of the resonance shapes. To ascertain that the ODMR signal was actually derived from the 1.911-eV triplet emission, the spectral dependence of the ODMR intensity was measured. In this case a fixed magnetic field was employed and the spectrum of ΔI was obtained by using a monochromator in front of the photomultiplier. As shown in Fig. 10 the spectrum of the microwave-induced PL signal at resonance is exactly the same as the 1.911-eV PL emission (Fig. 2). It can be seen that the tail from the COL emission (Fig. 1) does not contribute to the ODMR signal, confirming that this signal is only related to the 1.911-eV PL spectrum. It should be noted that the detailed structure obtained in the spectral dependence measurement allows independent confirmation of the assignment of the phonon replicas to the 1.911-eV system.

In Fig. 11 a spectrum from a level crossing measurement is shown. Here, the change in PL intensity upon variation of the magnetic field is detected with no microwave field applied. This measurement confirms that the resonances in the ODMR signal (Fig. 9) are due to a triplet exciton as illustrated in the level diagram for $\vec{B}||z$ in Fig. 12. The magnetic sublevels $| -1 \rangle$ and $| 0 \rangle$ cross for

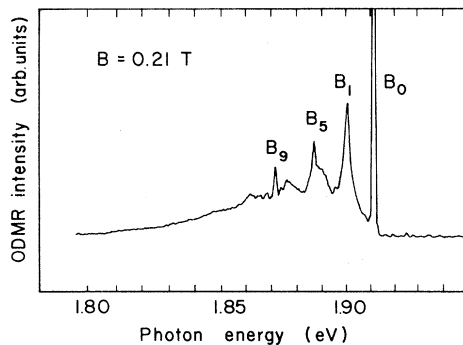


FIG. 10. Spectral dependence of the ODMR triplet resonance at high resolution (0.1 nm).

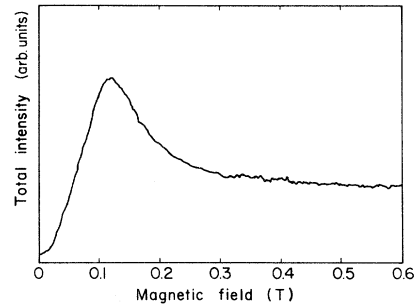


FIG. 11. Level crossing signal (ΔI vs B) for $\vec{B}||[001]$ and monitoring all of the emission.

a certain value of the magnetic field $\vec{B}||z$, in which case a mixing between these states occurs. For this direction of the magnetic field ($\vec{B}||z = \langle 001 \rangle$) the symmetry is not reduced below the crystal-field symmetry C_{4v} appropriate for a $\langle 001 \rangle$ -oriented defect. In Fig. 12 the BE levels are labeled according to the representation of this point group, and the allowed electric dipole transitions are shown. Transitions between the Γ_2 level and the ground state are forbidden in this symmetry. Therefore, both the I_{σ^-} component and the total emission intensity increase when the level crossing mixes the states. In spite of a small orthorhombic distortion of the center which relaxes the above selection rules an increase in the total emission intensity is obvious in Fig. 11. This provides an independent identification for the observation of an uncom-

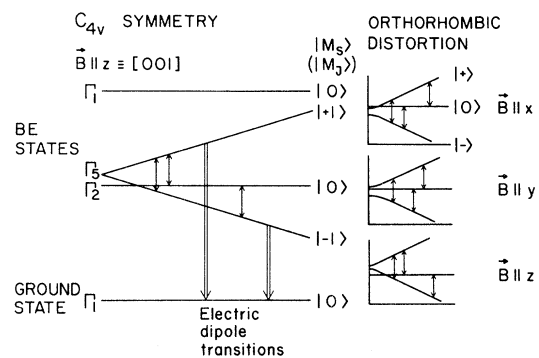


FIG. 12. (a) Energy-level scheme for C_{4v} symmetry assuming negligible orthorhombic distortion. The allowed electric dipole transitions are shown for $| +1 \rangle \rightarrow | 0 \rangle$ and $| -1 \rangle \rightarrow | 0 \rangle$. The $\Delta M_s = \pm 2$ is allowed only for $\vec{B}_{rf}||\vec{B}$ whereas the $\Delta M_s = \pm 1$ transitions are observed for the usual experimental arrangement with $\vec{B}_{rf} \perp \vec{B}$. (b) Energy-level schemes for an orthorhombic center with the magnetic field parallel to the principal directions, e.g., $[110] \equiv x$, $[011] \equiv y$, and $[001] \equiv z$.

pletely thermalized triplet system.¹⁸ We see no evidence of a hyperfine structure analogous to that observed by Lee *et al.*²⁷ in our case.

The Hamiltonian describing these bound exciton states in magnetic field \vec{B} is¹⁸

$$\mathcal{H} = \mu_B \vec{B} \cdot \vec{g}_{ex} \cdot \vec{S} + D[S_z^2 - \frac{1}{3}S(S+1)] + E(S_x^2 - S_y^2). \quad (1)$$

For an axial center (where E is small) the basis states are $|+1\rangle$, $|0\rangle$, and $|-1\rangle$, and the zero-field splitting between $|\pm 1\rangle$ and $|0\rangle$ states is determined by the parameter D . If an orthorhombic distortion is present as in this case, the last term in Eq. (1) has to be included. Then the two $|\pm 1\rangle$ states are also split in zero magnetic field and labeled $|\pm\rangle$. The three principal directions describing a $[001]$ defect are $x \equiv [110]$, $y \equiv [1\bar{1}0]$, and $z \equiv [001]$ and the corresponding energy-level schemes for the magnetic field parallel to these directions are shown in Fig. 12. If the system is unthermalized, the population differences between these energy levels are determined by the different decay rates from the levels. Thus the levels with high emission rates empty preferentially, and at resonance the microwaves induce transitions to these states from weakly emitting states. A similar situation occurs for partly thermalized systems. This is also illustrated in Fig. 12, where for the magnetic field along the major axis (z) of a defect the $|0\rangle$ state emission is weak. Two resonances are observed, as shown, $|0\rangle \rightarrow |+\rangle$ which increases the $I_{\sigma+}$ emission principally at low field and $|0\rangle \rightarrow |-\rangle$ which increases the $I_{\sigma-}$ emission at high field. These resonances are separated by $2D/g_{ex}\mu_B$ and the mean-field position gives g_{ex} .

The ODMR spectrum for GaP:Cu is more complicated than that observed in an axial crystal such as GaSe (Ref. 28) since it is clear that there will be a set of three axial defects for symmetry $\langle 001 \rangle$. For orthorhombic centers there will be six inequivalent defects and with each exciton giving two triplet resonances a total of 12 ODMR signals may be observed for an arbitrary angle between the magnetic field and the crystal axes. In the present case the ODMR spectrum for $\vec{B} \parallel [001]$ can be seen to contain two distinct pairs of lines since, as labeled in Fig. 9, two of the three sets of $\langle 100 \rangle$ centers remain degenerate; $[001] \parallel \vec{B}$, $[010] \perp \vec{B}$, and $[100] \perp \vec{B}$. The separation between the resonances is determined by the angles between the axes of the center and the magnetic-field direction. Observa-

tions of the ODMR spectra as \vec{B} was rotated in the $(1\bar{1}0)$ and (100) planes of the crystal confirmed that the resonances are due to $\langle 001 \rangle$ centers. The results for rotation in the $(1\bar{1}0)$ plane are shown in Fig. 13(a), where the solid lines have been calculated using the Hamiltonian in Eq. (1). Figure 13(b) shows the angular dependence for rotation in the (001) plane and a fit using Eq. (1). The corresponding spin-Hamiltonian parameters were found to be $g_x = 2.20 \pm 0.01$, $g_y = 1.95 \pm 0.01$, and $g_z = 2.05 \pm 0.01$, further $D = +0.013 \pm 0.001$ meV and $|E| = 0.0025 \pm 0.0006$ meV.

It is apparent in Fig. 13 that there is a low-field transition which shows only slight anisotropy. This is, in fact, the $\Delta M_s = \pm 2$ transition which is shown on the energy-level diagram (Fig. 12). The position of this line depends principally on the g value and since this is nearly isotropic, $g \approx 2$, the $\Delta M_s = \pm 2$ transition occurs near an effective $g = 4$. For $\vec{B} \parallel [001]$ this transition is very weak for the usual experimental arrangement (the oscillating rf field perpendicular to the z axis of the system) though it can be seen in Fig. 9. However, the in-

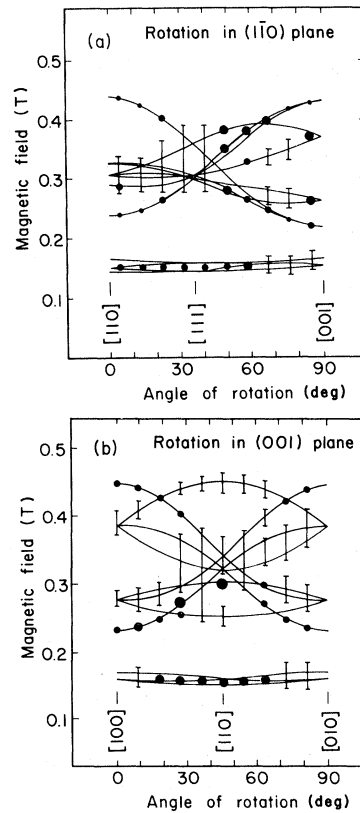


FIG. 13. Angular dependence of the triplet ODMR spectrum for rotation in the $(1\bar{1}0)$ plane and the (001) plane. The solid lines are calculated for orthorhombic symmetry with the parameters given in the text.

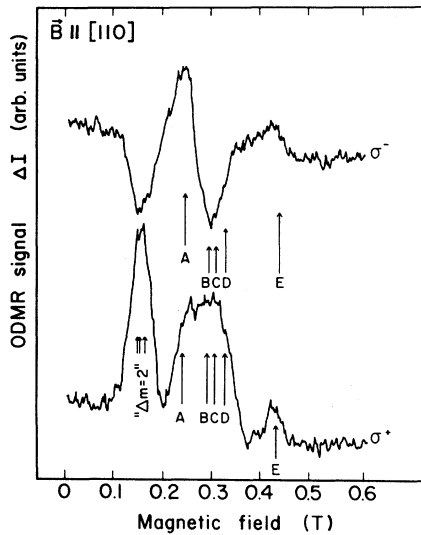


FIG. 14. An ODMR spectrum for $\vec{B} \parallel [110]$. When the magnetic-field orientation is away from the defect axis (the z direction) emission is allowed for all levels in Fig. 12 and population differences are small. Then all resonances are weak.

tensity of this line increases as \vec{B} is rotated away from the defect axis. This is obvious from Fig. 14 where an ODMR spectrum is shown for $\vec{B} \parallel [110]$. For \vec{B} away from the z direction the emission is allowed for each level so that population differences are small and all resonances are weak (Fig. 14). A small degree of thermalization and different decay rates from the $|+\rangle$ and $|-\rangle$ states account for the observation of the $\Delta M_s = \pm 2$ transition. Also, the sign of the D as positive is clear from the effect of thermalization on the magnitude of the ODMR signals (for $\vec{B} \parallel [001]$, $\Delta I_{\sigma+} > \Delta I_{\sigma-}$).

VI. DISCUSSION

The new information on the 1.911-eV center in GaP:Cu obtained in the present study illustrates the complexity of such deeply bound exciton systems, which behave quite differently from previously studied deep BE states in GaP, (e.g., Zn, O and Cd, O).^{14,15} The theory for bound-exciton states available in the literature¹⁷ is inadequate to explain the detailed electronic structure of the complex Cu defects responsible for the COL emission¹¹ and the 1.911-eV emission. We have therefore extended the previous generic theoretical models for exciton binding at axial centers to account for the observed electronic structure of the

1.911-eV center and use this to support tentative models for the identity of this defect in GaP:Cu.

Before discussing our models for the identity and electronic structure of the 1.911-eV center, a short review of the relevant experimental data available is helpful. The photoluminescence data in connection with the doping conditions give the information that Cu is involved, and that the electronic triplet observed at 1.911 eV has the characteristics of an exciton bound to a neutral associate (long luminescence lifetime). Attempts to prove possible association of Cu with other impurities have shown no connection with intentional or inadvertant dopants such as S, Te, O, N, or Zn. Further, isotope shifts are observed in the sharp phonon replicas of the 1.911-eV sideband when $^{63}\text{Cu} \rightarrow ^{65}\text{Cu}$ (Table I). These shifts are as large as 0.5 meV in the 24-meV replica, which is probably a locally perturbed LA mode. The presence of Cu in the complex is thus proved. Since the LA_X mode involves the motion of the Ga sublattice alone²⁹ the selectively largest isotope shift for a mode isoenergetic with LA normal modes of the GaP lattice suggests a Cu_{Ga} substituent.³⁰ The Zeeman measurements of the 1.911-eV line show an almost symmetric splitting into three components in magnetic field (Fig. 2). A nearly isotropic $g \approx 2$ is deduced from the angular dependence of the splitting. Partial thermalization of these three components in a magnetic field up to 6 T proves that the splitting occurs in the initial state of the luminescence transition, ruling out, e.g., a transition of an outer electron into a d -shell triplet of the Cu atom. Important complementary information is provided by the ODMR data, which show the $\langle 100 \rangle$ orientation of the symmetry axis. This illustrates the higher resolution of the ODMR measurements when the Zeeman analysis is unable to determine the symmetry of the center from the very small anisotropy of the recombination energies from the different magnetic substates of the triplet-bound exciton. The ODMR technique has greater sensitivity in this respect because transitions between the magnetic substates are measured directly, and the anisotropy is a much larger proportion of these energy separations.

The data discussed so far provide only results for the lowest state of the bound exciton, being based on low-temperature photoluminescence spectra. The temperature dependence of the emission intensity adds information on thermal activation energies of the particles involved in the transition. However, in this case the higher bound-exciton

states are separated too far in energy from the lowest state to become thermally populated before the emission is strongly broadened and quenched. Photoluminescence excitation spectroscopy on the other hand provides valuable results for the higher electron states of the bound exciton. This is a much more valuable method than optical absorption in the detection of weak absorption processes associated with a particular center in isolation from competing absorption from other centers. The linewidth of the transitions to these higher-energy states shown in Fig. 7 is lifetime broadened by transitions to lower-energy states. A very strong magnetic field would be needed to reveal the multiplicity of these high-energy components. However, by analogy with the COL center¹¹ these may well be predominantly due to magnetic singlet-exciton states as discussed below.

A model of the defect complex causing the 1.911-eV emission has to account for all the above-mentioned pieces of information. The model should include the local arrangement of Cu atoms in the center, as well as the electronic structure of the exciton bound at the center.

A. The electronic structure of the 1.911-eV bound exciton

From the Zeeman and ODMR data displayed in the previous sections it was concluded that the electronic structure of the 1.911-eV bound exciton depends on the axial symmetry of the center binding the exciton. The final state in the transition is the ground state of a neutral isoelectronic center having no spin, while the initial state of the bound exciton in emission is found to be an approximate spin triplet giving an almost isotropic g value $g \approx 2$. Similar behavior has been reported for several other centers^{17,31,32} where the isotropic behavior has failed to reveal the symmetry axis in the absence of ODMR data.

In a general model for the bound-exciton states these can be regarded as formed from electron states derived from the six $\langle 100 \rangle$ conduction-band minima and hole states derived from the uppermost valence-band maximum at Γ in the reduced Brillouin zone. For the present situation of relatively tightly bound electron states $E_e > 0.1$ eV, the camel's back splitting of the GaP conduction-band structure near symmetry point X in the Brillouin zone is negligible,¹⁷ and a simplified model with three isoenergetic minima centered on X is sufficient. The valley-orbit splitting of the threefold

degenerate linear combination of conduction-band states, induced by the localization of the electron in case of an attractive local potential, results in a lowest-lying Γ_6 (C_{4v} double group) bound-electron state with $m_j = \pm \frac{1}{2}$. A similar result can be deduced if a strong compressive axial field is the primary perturbation of the electron states as discussed below. The bound-hole states can be considered to be formed from p -like orbital states coupled with spin. The C_{4v} $\langle 001 \rangle$ -oriented axial crystal field splits the p states into a p_0 ($m_l = 0$) and a p_{\pm} ($m_l = \pm 1$) state, which when coupled with spin form $m_j = \pm \frac{1}{2}$ (Γ_6) and $m_j = \pm \frac{1}{2}, \pm \frac{3}{2}$ (Γ'_6, Γ_7) bound-hole states, respectively. In the limit of a strong axial field the spin-orbit coupling between the Γ_6 and Γ'_6 states is quenched and the Γ_6 state tends to behave as a pure-spin state. In the case of the 1.911-eV system we have observed magneto-optical behavior which is consistent with the lowest energy state of the bound exciton being the triplet state (effective spin $J = S = 1$) formed from the Γ_6 bound-hole and bound-electron states coupled by the Coulombic exchange interaction, thus:

$$\Gamma_6 \times \Gamma_6 = \Gamma_1 + \Gamma_2 + \Gamma_5 .$$

The Γ_1 state refers to a $S = 0$ singlet BE state and the $S = 1$ triplet consists of a Γ_5 ($M_s = \pm 1$) doublet and a Γ_2 ($M_s = 0$) singlet as shown in Fig. 12. The small value of the zero-field splitting of the $S = 1$ triplet state ($D = +0.013$ meV) confirms the almost pure-spin character of the bound particles.¹⁷

The splitting of the hole states discussed above, giving a lowest-lying Γ_6 bound-hole state, implies that the system experiences a strong compressional axial crystal field (as shown in Fig. 15). This is the most probable way of obtaining an attractive local potential for electrons as well as holes, a neglected possibility in earlier descriptions of these states.¹⁷ The sign of the axial field is opposite to the sign appropriate for, e.g., the Cd-O system in GaP,^{14,15} owing to the large ionic radii of the Cu_I atoms and the small radius of O_P. The spin-orbit splitting Δ_{so} of the GaP host is around 82 meV, whereas the axial field causes splitting on the order of 280 meV as shown in Fig. 15. Mixing of the hole wave function with the $3d$ states of Cu, which show inverted spin-orbit splitting, should reduce the local spin-orbit splitting of the bound-hole states,³³ or even result in a negative value compared to the GaP host. In any case the large axial field splitting dominates over the spin-orbit splitting as illustrated in the coupling scheme of Fig. 15.

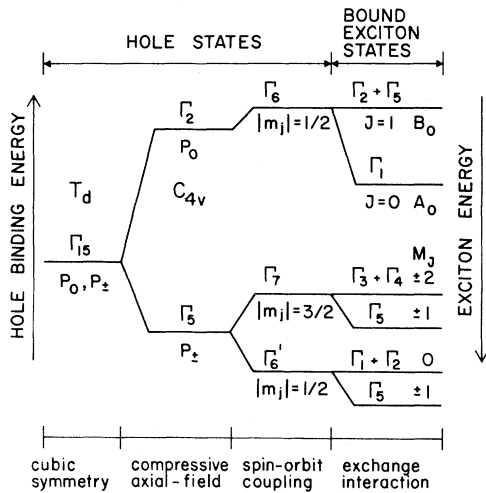


FIG. 15. Level diagram for the 1.911-eV bound exciton. To the left hole states are shown to split from the triply degenerate Γ_{15} representation into a p_0 singlet hole state (at highest hole binding energy for compressive-strain field) and a doubly degenerate p_{\pm} hole state. Adding the smaller spin-orbit coupling a pure-spin state Γ_6 has the highest hole binding energy while the p_{\pm} state splits into Γ_6' and Γ_7 doublets. To the right the bound-exciton states are shown. The combination of two pure-spin particles gives a singlet-triplet pair $J=0, 1$ where the triplet is the lowest BE state. The spin-forbidden 1.911-eV transition is between the triplet $J=1$ (highest in the diagram) and the spin-free ground state. The exceptionally large exchange splitting $\Delta_{JJ}=91$ meV is owing to a large overlap between the electron and hole wave functions in the hole-attractive central cell of the defect. This is possible through strain-induced contribution to the electron binding energy, compared with the Coulomb value predicted in the HTL model.

Comparing the level diagram in Fig. 15 with the experimental data in Figs. 2 and 7 the transition from the $J=1$ bound-exciton state (i.e., the effective spin $S=1$) to the ground-state singlet refers to the 1.911-eV electronic line seen in emission. This transition has a very low oscillator strength in excitation measurements, illustrating a spin-selection rule $\Delta S=0$, according to which the transition is forbidden. The strong line at 2.002 eV observed in PLE spectra corresponds to a transition between the ground state and the $J=0$ bound-exciton state. This interpretation requires a large exchange splitting of $\Delta_{JJ}=91$ meV, exceptional for BE in semiconductors. A J - J coupling of this size implies an unusual degree of overlap and therefore a strong exchange interaction between the electron and hole of the bound exciton in the vicinity of the central

cell containing the associate. The COL center which is believed to be a triple Cu associate exhibits a smaller but also unusually large exchange splitting.¹¹ In agreement with the increased exciton binding energy of the 1.911-eV center (0.44 eV) compared with the COL (0.18 eV), and hence generally more localized wave functions, the exchange splitting Δ_{JJ} is much larger for the former; $\Delta_{JJ}=91$ meV for the 1.911-eV center but $\Delta_{JJ}=23.2$ meV for the COL.

Cu is known to create deep acceptor states in GaP, 0.5 and 0.7 eV from the valence-band edge.⁴ The centers causing the acceptor levels are not identified but presumably Cu_{Ga} is involved, perhaps in a complex with other defects for at least one of these two centers. Hence, it may be concluded that the hole is also very tightly bound to the isoelectronic center suggested here if the hole wave function is mainly localized on an acceptorlike associate containing Cu_{Ga} , [for example, the $(\text{Cu-Ga})_{\text{Ga}}$ split interstitial discussed below]. The BE states involved are deep compared to effective-mass theory and the exciton is strongly localized at the defect. Also as discussed above, the hole states are strongly perturbed by the local axial field compared with the host states.

A key to the understanding of the large electron-hole overlap observed for excitons bound to the Cu complexes discussed above is to consider the effect of the strong local strain field on the electron states as well as the hole states. Through the presence of Cu_{Ga} , as mentioned above, the hole is strongly bound in the hole-attractive central-cell potential of Cu. Apparently the electron is also tightly bound with an energy much larger than predicted by the Hopfield-Thomas-Lynch (HTL) model¹⁶ for the binding energy of electrons in a Coulomb potential as second particles at hole-attractive neutral (isoelectronic) centers. A maximum value of 45–50 meV is expected for the electron binding energy in the case of GaP according to the HTL model. However, the thermal activation data indicate that neither particle of the BE takes less than about 120 meV of the total exciton binding energy of 440 meV for the 1.911-eV center.

Therefore, we postulate that the compressional local strain field increases the binding energy of the electron states as well as the $m_j = \pm \frac{1}{2}$ hole states which are split from the top of the valence band to produce a large hole binding energy under this sign of the axial field. This effect of the compressional strain field is opposite to the previ-

ously reported examples of neutral complexes involving small substitutional species such as N or O. This strain-induced contribution to the electron binding energy of a center with a strong hole-attractive central cell as Cu_{Ga} is responsible for the unusually large electron-hole overlap in the vicinity of the defect.

The local strain-induced attraction for the electron can be partly caused by a hydrostatic effect of the compressive strain which shifts the center of gravity of the electron states towards lower energies along with the band gap for compression.³⁴ If the defect axis is not oriented along a $\langle 111 \rangle$ direction, which is equivalent for all three $\langle 001 \rangle$ conduction-band minima of GaP, the crystal field causes splitting of the multivalley degenerate electron states. For an electron-attractive center in cubic symmetry the lowest state is generally a $1sA_1(\Gamma_6)$ state,^{29,31} which is unsplit by an axial strain field. This is also the case for bound-electron states at the more electron-attractive P site in GaP. However, if the axial strain energy exceeds the valley-orbit energy of the electron states, the electron ground state will be an s envelope state from only the $\langle 100 \rangle$ pair of valleys for stress parallel to $\langle 100 \rangle$.

In cubic symmetry a $1sE(\Gamma_8)$ state which is magnetically a pure-spin state¹⁷ is separated from the Γ_6 ground state by the valley-orbit splitting. This state will split into a pair of doublets in an axial strain field away from the $\langle 111 \rangle$ direction in GaP. An inverted V-O splitting occurs if the electron is bound in a locally repulsive potential.

If the lowest electron state is a $1sT_2$ state as in the case of a donor on the less electron-attractive Ga site²⁹ there will be a small spin-valley splitting of the $1sT_2$ state, resulting in a Γ_7 doublet and a fourfold degenerate Γ_8 state in cubic symmetry.³¹ The spin-valley splitting is likely to be a negligible feature, however, for the cases of large dominating strain splitting discussed in this paper. Instead, the triply degenerate T_2 electron states split into a singlet and a doublet with the former at lower energy for compression. Therefore, a pure-electron spin state is formed just as for the holes in an axial strain field under this sign. This is required to account for the observed case of a singlet-triplet pair of BE states with large overlap between the particle wave functions.

A detailed model for the 1.911-eV center is still tentative. It is not clear which of the above cases would be most appropriate for the electron-binding problem. However, the increased electron-binding

energy at the center will result from those components of the electron states which are lowered by the compressional axial field of the defect. In view of the very large exchange interaction between the particles of the bound exciton, it is concluded that the electron wave function is most probably symmetric around the impurity site.

We believe that strain-induced contribution to the binding energy of electrons at neutral isoelectronic associates which produce compressional strain fields is a general result for such defects. In the case of Cu-Li complexes, which appear after a second Li diffusion of GaP:Cu, a complex BE structure involving a singlet-triplet pair is assigned to a splitting of the electron states by a compressional axial strain field in a similar way as discussed above.²³ Here the BE states are subject to the same sign of the axial-strain field as the Cu complexes giving the 1.911 eV and the COL emissions. However, the magnitude is much smaller due to the smaller Li atoms replacing Cu in the complexes.²³ Also the axial center $\text{Sb}_P\text{-Sb}_P$ in GaP (Ref. 32) shows two singlet-triplet pairs of BE lines. The basic electron states are here assumed to be $1s(E)$, since the Sb_P core is attractive to holes and the valley-orbit splitting characteristic of the P sublattice in GaP will be inverted. The $1s(E)$ state can split in the $\langle 110 \rangle$ -oriented compressional field of this defect to produce, together with the $s = \frac{1}{2}$ hole, the two pairs of $J=0$ and $J=1$ states observed.²³

The electronic line C_0 , 280 meV above the 1.911-eV transition, is attributed to transitions to bound-exciton states derived from the p_{\pm} split-off hole states (Fig. 15). This gives roughly the size of the axial field splitting, neglecting Δ_{so} . A lifetime broadening of the C_0 component is consistent with rapid excitation transfer to lower bound-exciton states or to continuum states where one particle is ionized. The A_0 line is also lifetime broadened. At this point the details of the higher-energy components are not firmly established. The level scheme presented, however, accounts for the basic properties of the 1.911-eV bound exciton, consistent with the identification of the center binding the exciton as being a linear $\langle 100 \rangle$ -oriented defect.

B. The identity of the 1.911-eV center

It has proved to be a difficult task to obtain a unique microscopic model for the defect binding the 1.911-eV exciton. Although the generic model for the binding mechanism in the case of local attraction for both electrons and holes has been es-

tablished as presented above, we can still only be tentative about our microscopic model despite knowing the defect symmetry.

The careful isotope and doping studies made in this investigation, and also by Wight *et al.*,²² imply that the 1.911-eV center involves Cu without correlation to other intentional dopants. However, native defects can neither be revealed by isotope measurements nor by chemical doping studies and must therefore be considered as possibly involved in the defect. Neutral Cu has the electronic configuration $3d^{10}4s$ and is therefore lacking two valence electrons to complete the local bonds to the phosphorus neighbors when replacing Ga $3d^{10}4s^24p$. Also, Cu can act as an interstitial donor: $\text{Cu}^+ 3d^{10} + e^- 4s$.

Hence, if a complex is to be neutral and only consist of Cu atoms with complete d shells it has to involve three atoms. This is the case for the COL center, where a $\text{Cu}_I\text{-Cu}_{\text{Ga}}\text{-Cu}_I$ defect was found to correspond to the observed properties of that center.¹¹ All three Cu atoms then have the $3d^{10}$ configuration and the substitute is neutral in the sense that all valence-bond requirements are fulfilled in the neutral-charge state. The $\text{Cu}_I\text{-Cu}_{\text{Ga}}\text{-Cu}_I$ center might then be described as isoelectronic in the sense that it provides the same valence bonding as the Ga atom replaced, though of course it is not isoelectronic with respect to the total electron configuration, including the inner shells. However, the neutral center has no unpaired electronic spin and all inner shells are complete. The considerable differences in phonon coupling between the COL Cu complex and the 1.911-eV complex will have to be understood in terms of the model for the defect identity. It has been suggested that the complicated low-energy-mode structure observed for the COL emission as discrete replicas at 5.3, 6.8, and 8.8 meV from the electronic line^{11,19} is due to vibrations of the two interstitial Cu atoms. The 10.3-meV B_1 mode of the 1.911-eV emission does not seem to be comparable to these low-energy COL modes, since it shows no Cu isotope shift (Table I). Compared with the COL the B_1 mode lies close to an energy region in which coupling to much higher density of states of lattice modes may dilute the fractional kinetic energy of the Cu ions sufficiently to make the isotope shift hard to measure. However, the complete absence of an isotope shift suggests that the B_1 mode does not involve the motion of Cu and the model with Cu atoms only has to be rejected for the 1.911-eV center.

Models including a native defect seem to give better agreement with the observed properties of the 1.911-eV center. Considering the observed lack of correlation with all the likely impurity species, a plausible interstitial component for the 1.911-eV center may be Ga_I . The ionization energies of atomic species suggest that Ga_I would contribute only one electron to the local bonding of the associate. Then a simple possibility for the associate is a Cu-Ga_I pair defect. For completing the bonds to the neighboring P atoms this defect must either accept an electron if the Cu atom is to be in the $3d^{10}$ configuration (a charged center), or else the Cu has an unfilled d shell ($3d^9$). In the latter case the center is neutral and can in principle be viewed as a neutral acceptor, since it is negatively charged upon electron capture. The unfilled d shell implies that the $\text{Cu}_{\text{Ga}}\text{-Ga}_I$ center has a magnetic moment and the ground state of the neutral center will not be a $J=0$ state as required for an isoelectronic center. It is possible, though, that the overlap between the d^9 hole and the electronic particles in the BE is sufficiently small to give negligible magnetic coupling, so that the d^9 hole remains unaltered during the BE recombination. A crystal-field ground state of $3d^9$ well below the top of the valence band provides a possible configuration for such a case. This could in fact also be consistent with weak overlap between the d^9 hole and the valence band to give a weak Auger process. Normally strong Auger effects are expected upon the recombination of a tightly bound exciton at a center binding more than two electronic particles.³⁵ The very long decay time observed for the 1.911-eV emission is in contradiction to the presence of any Auger effects. Therefore, the two $4s$ electrons left on the Ga_I atom are probably a more serious problem in view of the absence of Auger effects at the 1.911-eV center. Magnetically though, the two electrons would couple to give a total spin of zero. Also the high Cu diffusion temperature required to produce the 1.911-eV system might indicate that Ga_I is indeed involved.

If the 1.911-eV center is simply a $\text{Cu}_{\text{Ga}}\text{-Ga}_I$ pair defect the interstitial atom would need to be on the tetrahedral site surrounded by P atoms in agreement with the $\langle 100 \rangle$ -oriented defect axis determined by the ODMR measurements. This is shown in Fig. 16(a).

Other types of defects with this specific symmetry axis include $\langle 100 \rangle$ -split interstitial pairs such as $(\text{Cu-Cu})_{\text{Ga}}$ or $(\text{Cu-Ga})_{\text{Ga}}$. Combined with a native interstitial species such as Ga_I along the same

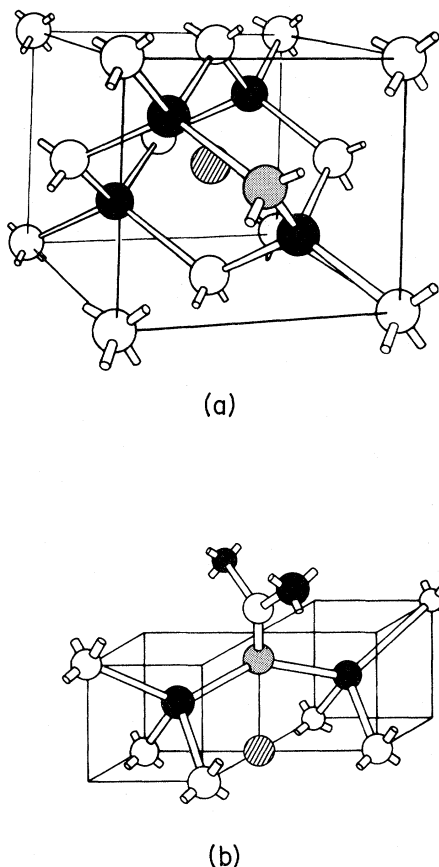


FIG. 16. (a) $\text{Cu}_{\text{Ga}}\text{-D}_1$ pair oriented in the $\langle 100 \rangle$ direction is a possible configuration of the defect binding the 1.911-eV exciton in GaP. The black atoms are phosphorous atoms and the white ones gallium atoms while Cu is shown dotted. The interstitial atom (presumably a Ga_I) is located on a tetrahedral site surrounded by four P atoms. (b) Another possible configuration of the 1.911-eV center in GaP. The black atoms are phosphorous atoms, while the white ones are Ga atoms. Cu is shown as dotted. The $(\text{Cu-Ga})_{\text{Ga}}$ forms a split $\langle 100 \rangle$ interstitial pair, which is stabilized by an interstitial atom adjacent to the Cu_{Ga} atom, providing an electron to complete the valence bonds. This interstitial atom is possibly Ga_I .

direction, these possess both the correct orientation and account for the lack of isotope shift in the 10-meV phonon mode. In the $(\text{Cu-Ga})_{\text{Ga}}$ case strong mixing of Cu and Ga motion should occur, leading to an isotope shift in the 24.2-meV mode as required. The Cu atom would in this case have a complete d shell, since the split interstitial pair on a Ga site needs just five electrons to fulfill local bonding requirements. This model suffers from the disadvantage that the $(\text{Cu-Ga})_{\text{Ga}}$ split intersti-

tial would seem likely to be weakly metastable against the configuration $\text{Cu}_I\text{-Ga}_{\text{Ga}}$, unless the split interstitial would be stabilized by the Ga_I in the arrangement $\text{Ga}_I\text{-(Cu-Ga)}_{\text{Ga}}$. This associate is shown in Fig. 16(b).

Since Ga is unlikely to contribute more than one electron to the local bonding, both Cu atoms are in the divalent charge state ($3d^9$) if the center is $(\text{Cu-Cu})_{\text{Ga}}\text{-Ga}_I$. Therefore, a simpler possibility is indeed $\text{Cu}_{\text{Ga}}\text{-Ga}_I$, where again the Cu_{Ga} involves a $3d^9$ hole which would have to be magnetically inactive in the BE transition as discussed above. This last model may be the most consistent with the relatively straightforward vibronic-mode structure of the 1.911-eV center although the absence of Auger effects seems difficult to understand if Ga_I is involved.

In addition, on this model it may also be possible to account for the substantial change of E_{BX} between the 1.911 eV and the COL (Ref. 11) centers. This shift can receive a rather simple explanation on an electrostatic (ionic) model, if the 1.911-eV center is simply $\text{Cu}_{\text{Ga}}\text{-Ga}_I$, whereas the COL is $\text{Cu}_I\text{-Cu}_{\text{Ga}}\text{-Cu}_I$. Then, the additional interstitial donor would be expected to produce a substantial reduction in the hole binding energy at the COL compared with the 1.911-eV center.

VII. CONCLUSIONS

The BE emission bands introduced into GaP upon Cu diffusion under proper conditions have been the subject of a systematic optical study, including the investigations of the 1.911-eV bound exciton reported here. Together with the COL bound exciton at 2.1774 eV, the 1.911-eV BE exhibits several unusual properties, which seem to be characteristic for excitons bound to Cu complexes in GaP.^{11,19,30} However, it is argued here that the very large exchange splitting Δ_{JJ} exhibited by these bound excitons may be a general result for an associate with a large locally compressive axial strain contribution to the electron binding provided that the central-cell potential is also strongly attractive for a hole. The activation energy for the thermal quenching of the BE luminescence of 120 meV reported here also supports the conclusion from the large Δ_{JJ} that the electron and hole are *both* bound by large energies to this associate.

The results of this work have necessitated a reconstruction of the theory of exciton binding at neutral centers in semiconductors. The general model developed here for the case of a large

compressional local axial field represents a significant extension of previous concepts. Although such phenomena may be expected for centers other than those associated with Cu, it may be that the activity of Cu as a fast-migrating interstitial species makes it exceptionally likely to promote associates with large compressional strain.

A spin-selection rule is indicated in the PLE spectrum suggesting that the lowest state is a relatively pure-spin triplet, consistent with the exceptionally large crystal-field and exchange splittings and yet small zero-field splitting of the $|\pm 1\rangle$ and $|0\rangle$ substrates of the triplet. A similar though less rigid selection rule has been observed for the COL Cu-related center in GaP.¹¹

The 1.911-eV BE emission is observed only after Cu diffusion at high temperatures, about 1050°C, when the temperature is rapidly quenched after a typical diffusion time of about 1 h. Attempts to relate this BE to any other dopants have failed as also observed in previous doping experiments.^{8,22} The presence of Cu in the defect complex is therefore concluded from the doping procedure as well as isotope shifts of some phonon replicas when substituting ⁶³Cu for ⁶⁵Cu. The absence of isotope shift for the dominating 10-meV phonon replica in the emission spectrum, on the other hand, suggests that other species besides Cu are also involved. In view of the doping results Ga_I is proposed as the additional part of the associate. In agreement with

the defect symmetry determined from ODMR measurements it is concluded that the linear $\langle 100 \rangle$ -oriented (Cu-Ga)_{Ga} split interstitial is likely to be responsible for the 1.911-eV emission, as a neutral associate with filled *d* shell when paired with a Ga_I donor. This defect is consistent with the fact that two electrons are needed to compensate Cu_{Ga} when forming a neutral center. Alternatively a (Cu-Cu)_{Ga}-Ga_I or a Cu_{Ga}-Ga_I associate where the Cu atoms have unfilled *d* shells may be considered as the identity of the 1.911-eV center. On this model, the magnetic properties of the *d*⁹ configuration must remain unaltered in the transition. This is reasonable if the 3*d*⁹ state of Cu⁺² lies well below the top of the valence band in GaP.³⁶ In all cases, the Ga_I would need to be in the tetrahedral site surrounded by P atoms to maintain the $\langle 100 \rangle$ -oriented symmetry. Alternative models seem inconsistent with the absence of a Cu isotope shift in the dominant low-energy phonon replica and no spin in the final state of the recombination.

In conclusion we note that further progress in the understanding of these remarkable spectra begs the question of a detailed understanding of the form of the phonon coupling in both the 1.911-eV and COL centers. In particular, the reason for the considerably weaker phonon coupling of the 1.911-eV spectrum despite larger exciton localization energy E_{BX} , requires an explanation.

¹See, e.g., H. J. Queisser, *Solid State Electron.* **21**, 1405 (1978), and references therein.

²A. G. Milnes, *Deep Impurities in Semiconductors* (Wiley, New York, 1973), p. 16.

³F. Willman, D. Bimberg, and M. Blätte, *Phys. Rev. B* **7**, 2473 (1973).

⁴H. G. Grimmeiss, B. Monemar, and L. Samuelson, *Solid State Electron.* **21**, 1505 (1978).

⁵A. A. Bergh and P. J. Dean, *Light Emitting Diodes* (Clarendon, Oxford, 1976).

⁶F. A. Kröger, *The Chemistry of Imperfect Crystals* (North-Holland, Amsterdam, 1964).

⁷J. A. Van Vechten, in *Handbook of Semiconductors*, edited by S. P. Keller (North-Holland, Amsterdam, 1980), Vol. 3, Chap. 1.

⁸P. J. Dean, *J. Lumin.* **7**, 51 (1973).

⁹D. V. Lang, *J. Appl. Phys.* **45**, 3023 (1974).

¹⁰J. A. Van Vechten, C. M. Ransom, and T. J. Chappell, in *Proceedings of the 15th International Conference on the Physics of Semiconductors, Kyoto, 1980* [*J. Phys. Soc. Jpn.* **49**, Suppl. A, 251 (1980)].

¹¹B. Monemar, H. P. Gislason, P. J. Dean, and D. C.

Herbert, *Phys. Rev. B* **25**, 7719 (1982).

¹²S. Depinna, B. C. Cavenett, N. Killoran, and B. Monemar, *Phys. Rev. B* **24**, 6740 (1981).

¹³M. D. Sturge, E. Cohen, and K. F. Rodgers, *Phys. Rev. B* **15**, 3169 (1977).

¹⁴C. H. Henry, P. J. Dean, and J. D. Cuthbert, *Phys. Rev.* **166**, 757 (1968).

¹⁵C. H. Henry, P. J. Dean, D. G. Thomas, and J. J. Hopfield, *Proceedings of the Conference on Localized Excitons in Solids, Irvine, California, 1967*, edited by R. F. Wallis (Plenum, New York, 1968), p. 267.

¹⁶J. J. Hopfield, D. G. Thomas, and R. T. Lynch, *Phys. Rev. Lett.* **17**, 312 (1966).

¹⁷P. J. Dean and D. C. Herbert, in *Topics in Current Physics*, edited by K. Cho (Springer, Berlin, 1979), Vol. 14, p. 55.

¹⁸B. C. Cavenett, *Adv. Phys.* **30**, 475 (1981).

¹⁹H. P. Gislason, B. Monemar, P.-O. Holtz, P. J. Dean, and D. C. Herbert, *J. Phys. C* (in press).

²⁰R. N. Bhargava, S. K. Kurtz, A. T. Vink, and R. C. Peters, *Phys. Rev. Lett.* **27**, 183 (1971).

²¹P. J. Dean, *Solid State Commun.* **9**, 2211 (1971).

- ²²D. R. Wight, J. W. A. Trussler, and W. Harding, *Proceedings of the Eleventh International Conference on the Physics of Semiconductors, Warsaw, 1972*, edited by M. Miasek (PWN—Polish Scientific, Warsaw, 1972), p. 1091.
- ²³B. Monemar, H. P. Gislason, P. J. Dean, S. Depinna, and B. C. Cavenett (unpublished).
- ²⁴P. J. Dean, *Phys. Rev. B* **4**, 2596 (1971).
- ²⁵A. A. Maradudin, in *Solid State Physics*, edited by F. Seitz and D. Turnbull (Academic, New York, 1966), Vol. 18, p. 273.
- ²⁶J. L. Yarnell, J. L. Warren, R. G. Wenzel, and P. J. Dean, *Neutron Inelastic Scattering* **1**, 301 (1968).
- ²⁷K. M. Lee, Le Si Dang, G. D. Watkins, and W. J. Choyke, *Solid State Commun.* **37**, 551 (1981).
- ²⁸K. Morigaki, P. Dawson, and B. C. Cavenett, *Solid State Commun.* **28**, 829 (1978).
- ²⁹T. N. Morgan, *Phys. Rev. Lett.* **21**, 819 (1968).
- ³⁰P. J. Dean, B. Monemar, H. P. Gislason, and D. C. Herbert, *Proceedings of the 1981 International Conference on Luminescence ICL, Berlin* [*J. Lumin.* **24/25**, 401 (1981)].
- ³¹P. J. Dean, W. Schairer, M. Lorenz, and T. N. Morgan, *J. Lumin.* **2**, 343 (1974).
- ³²P. J. Dean, R. A. Faulkner, and E. G. Schönherr, *Proceedings of the Tenth International Conference on the Physics of Semiconductors, Cambridge, 1970*, edited by S. P. Keller, J. C. Hensel, and F. Stern (U.S. Atomic Energy Commission, Oak Ridge, Tenn., 1970), p. 286.
- ³³D. J. Robbins, D. C. Herbert, and P. J. Dean, *J. Phys. C* **14**, 2859 (1981).
- ³⁴J. L. Merz, A. Baldereschi, and M. A. Sergent, *Phys. Rev. B* **6**, 3082 (1972).
- ³⁵D. J. Robbins and P. J. Dean, *Adv. Phys.* **27**, 499 (1978).
- ³⁶L. A. Hemstreet, *Phys. Rev. B* **22**, 4590 (1980).